Acta Pharmacologica Sinica 2017: 1048–1058
 1671-4083/17
www.nature.com/aps

Original Article

Diallyl trisulfide suppresses tumor growth through the attenuation of Nrf2/Akt and activation of p38/JNK and potentiates cisplatin efficacy in gastric cancer treatment

Xiao-yan JIANG[1], Xiao-song ZHU[1], Hong-ya XU[1], Zhong-xi ZHAO[1, 2, 3, *], Si-ying LI[1, *], Shan-zhong LI[3], Jian-hua CAI[3], Ji-min CAO[3]

[1]*School of Pharmaceutical Sciences, Shandong University, Ji-nan 250012, China;* [2]*Shandong Provincial Key Laboratory of Mucosal and Transdermal Drug Delivery Technologies, Shandong Academy of Pharmaceutical Sciences, Ji-nan 250101, China;* [3]*Jiangsu Shengshi Kangde Biotech Corporation, Lianyungang 222006, China*

Abstract

Diallyl trisulfide (DATS), a garlic organosulfide, has shown excellent chemopreventive potential. Cisplatin (DDP) is widely used to treat solid malignant tumors, but causing serious side effects. In the current study, we attempted to elucidate the chemopreventive mechanisms of DATS in human gastric cancer BGC-823 cells *in vitro*, and to investigate whether DATS could enhance the anti-tumor efficacy of DDP and improve quality of life in BGC-823 xenograft mice *in vivo*. Treatment with DATS (25–400 μmol/L) dose-dependently inhibited the viability of BGC-823 cells *in vitro* with an IC_{50} of 115.2±4.3 μmol/L after 24 h drug exposure. DATS (50–200 μmol/L) induced cell cycle arrest at G_2/M phase in BGC-823 cells, which correlated with significant accumulation of cyclin A2 and B1. DATS also induced BGC-823 cell apoptosis, which was accompanied by the modulation of Bcl-2 family members and caspase cascade activation. In BGC-823 xenograft mice, administration of DATS (20–40 mg·kg^{-1}·d^{-1}, ip) dose-dependently inhibited tumor growth and markedly reduced the number of Ki-67 positive cells in tumors. Interestingly, combined administration of DATS (30 mg·kg^{-1}·d^{-1}, ip) with DDP (5 mg/kg, every 5 d, ip) exhibited enhanced anti-tumor activity with fewer side effects. We showed that treatment of BGC-823 cells with DATS *in vitro* and *in vivo* significantly activated kinases such as p38 and JNK/MAPK and attenuated the Nrf2/Akt pathway. This study provides evidence that DATS exerts anticancer effects and enhances the antitumor efficacy of DDP, making it a novel candidate for adjuvant therapy for gastric cancer.

Keywords: diallyl trisulfide; cisplatin; human gastric cancer; cell cycle arrest; apoptosis; enhanced efficacy; Nrf2/Akt; p38/JNK

Acta Pharmacologica Sinica (2017) 38: 1048–1058; doi: 10.1038/aps.2016.176; published online 27 Mar 2017

Introduction

Gastric cancer is one of the most common cancers; it is widespread in many developing countries and is associated with high mortality[1]. Despite recent advances in identifying the tumorigenic mechanism of gastric cancer, the ever-expanding incidence and relatively low relief rate of chemotherapy has led to identification of a more efficacious treatment method.

Garlic (*Allium sativum* L) has been used for centuries as a prophylactic and therapeutic medicinal agent. Consumption of garlic is associated with a reduced incidence of gastric cancer[2]. Diallyl trisulfide (DATS), an oil-soluble compound extracted from garlic, has a variety of pharmacological and biological activities, including anti-inflammatory, antimicrobial, and antitumor activities[3]. The inhibitory effect of DATS on tumor growth involves multiple mechanisms, such as induction of reactive oxygen species[4], cell cycle arrest, promotion of apoptosis, suppression of proliferation[5], and inhibition of tumor cell invasion and metastasis[6]. Therefore, DATS may play an important role in cancer treatment as a chemotherapeutic agent.

The current major therapeutic modality for gastric cancer is chemotherapy plus surgical removal. Cisplatin (dichlorodiamino platinum, DDP) is an inorganic platinum-based chemotherapeutic agent that is widely used in the treatment of a variety of solid malignant tumors. The use of cisplatin is

*To whom correspondence should be addressed.
E-mail zxzhao@sdu.edu.cn (Zhong-xi ZHAO);
li-siying@hotmail.com (Si-ying LI)
Received 2016-07-21 Accepted 2016-12-24

frequently limited due to various significant side effects, such as immune system disorders, acute kidney injury, and induction of inflammation[7]. Evidence has shown that garlic and its derivatives can ameliorate cisplatin-induced nephrotoxicity and oxidative stress in male rats[8]. In addition, garlic has been suggested to significantly enhance immune system function. Recent studies have suggested that garlic acts as an immune booster by actively strengthening the host immune system within the tumor microenvironment against the immunosuppressive activity of the emerging tumor[9]. Based on these results, garlic-related compounds may be administered as dietary supplements in combination with DDP to provide synergistic effects or to ameliorate side effects.

The present study was designed to evaluate the possible therapeutic mechanisms of DATS on gastric cancer treatment *in vitro* and *in vivo*. Furthermore, we investigated whether DATS, in combination with DDP, enhanced anti-tumor efficacy and improved quality of life in xenograft mice.

Materials and methods

Materials

Diallyl trisulfide (DATS, 98% purity) was obtained from Aike Reagent Company (Chengdu, China). Cisplatin (DDP) was purchased from Qilu Pharmaceutical Co, LTD (Ji-nan, China). Sulforhodamine B (SRB), propidium iodide (PI) and anti-NQO1 antibody were purchased from Sigma–Aldrich (St Louis, MI, USA). Primary antibodies against cyclin A2, cyclin B1, cyclin E1, PCNA, Bax, Bcl-2, Bcl-xl, p53 and cytochrome *c* were obtained from Abcam (Cambridge, UK). Primary antibodies against Caspase-3/-7/-8/-9, cleaved Caspase-3/-7/-8/-9, cleaved PARP, ERK, p-ERK, JNK, p-JNK, p38 and p-p38 antibodies were purchased from Cell Signaling Technology (Danvers, MA, USA). Anti-Nrf2, anti-Akt and anti-p-Akt antibodies were obtained from Santa Cruz Technology (Heidelberg, Germany). Other reagents were purchased from Sigma–Aldrich (St Louis, MI, USA).

Cell culture and cell viability

BGC-823 and GSE-1 cell lines were provided by the Department of Pharmacology, Shandong University (Ji-nan, China) and cultured in RMPI-1640 (GIBCO, New York, USA) supplemented with 10% fetal bovine serum (FBS) at 37 °C in a 5% CO_2 humidified incubator. The sulforhodamine B (SRB) assay was performed as described previously to measure BGC-823 and GSE-1 cell viability after DATS treatment. Briefly, 3.0×10^3 cells/well were grown in 96-well plates for 12 h and exposed to different concentrations of DATS (0–400 μmol/L) for 24 or 48 h. The inhibition rate was calculated as a percentage of absorbance $(A_{con}\text{-}A_t)/A_{con}$. Three independent experiments were performed.

Cell cycle analysis

BGC-823 cells (2.5×10^5 cells/sample) were seeded in 6-well plates and incubated with DATS (50, 100 or 200 μmol/L) for 24 h. Cells were harvested and fixed in ice cold 70% ethanol at -20 °C overnight, then stained with 50 μg/mL PI for 30 min in the dark. Cell cycle progression was analyzed by a Beckman Coulter model FC 500 flow cytometer (Brea, CA, USA).

Apoptosis analysis

For quantitative analysis of apoptosis, BGC-823 cells were analyzed using an Apoptosis Detection Kit (Invitrogen, Carlsbad, USA). In brief, 2.5×10^5 cells/sample were treated with DATS (50, 100 or 200 μmol/L) for 24 h and were harvested and labeled with Annexin V and propidium iodide (PI) in accordance with the manufacturers' instructions.

Animal and tumor xenograft model

Six-week-old female BALB/c nude mice were purchased from the Institute of Laboratory Animal Sciences, Cams&Pumc (Beijing, China, SCXK 2014-0004; SYXK 2013-0001), and were housed under pathogen-free conditions with a 12 h light/12 h dark schedule and fed an autoclaved diet and water. All procedures were approved by the guidelines of the Ethical Committee Experimental Animal Center of Shandong University (No 2016020, Ji-nan, China).

To establish gastric carcinoma xenograft tumors in mice, BGC-823 cells (5.0×10^6) were suspended in 100 μL PBS and subcutaneously injected into the mice. The mice were sacrificed a month later. The tumor was separated by 2 mm fragments and implanted into other mice. When tumor volumes reached approximately 100 mm^3, mice were randomized and assigned to the following treatments: control (normal saline, containing 20% β-cycloamylose, every day); cisplatin (5 mg/kg, positive control, every 5 d); treated groups (DATS was formed with β-cycloamylose and dissolved in normal saline, dosage at 20, 30 or 40 $mg\cdot kg^{-1}\cdot d^{-1}$); and the co-treated group (cisplatin, 5 mg/kg every 5 d and DATS at 30 mg/kg all other days). Tumor diameter and body weight was recorded every three days starting from the first day of treatment. The tumor volumes were calculated using the following formula: $length\times width^2\times0.5$. All mice were sacrificed on the 32nd day, and the tumors were excised for weight measurement and histopathological analysis.

Histopathology and TUNEL assay

For histopathological analysis, the tumors and major organs (liver, lung, kidney, and spleen) were fixed in 10% neutralized buffered formalin and embedded in paraffin. Sections with a thickness of 4 μm were then stained with hematoxylin and eosin (H&E) solution.

In situ cell apoptosis was evaluated using a terminal deoxynucleotidyl transferase (TdT)-mediated dUTP nick end labeling (TUNEL) kit (Roche, Mannheim, Germany) following the manufacturer's protocol. Briefly, paraffin sections were deparaffined with xylene and rehydrated in a graded series of ethanol. After permeabilization with proteinase K, sections were incubated with labeled solution (labeled nucleotides and TdT enzyme) for 60 min and converter-POD solution for 30 min at 37 °C. Finally, sections were incubated with horseradish peroxidase-streptavidin and the peroxidase substrate 3'-diaminobenzidine (DAB; DAKO, Carpenteria, CA, USA) and then

counterstained with hematoxylin. Only heavily stained cells were considered to be apoptotic.

Ki-67 immunohistochemistry

Sections with a thickness of 4 μm were deparaffinized, rehydrated, and blocked in 10% bovine serum albumin. Sections were then incubated with anti-Ki-67 antibody overnight. Binding of primary antibodies was detected with a horseradish peroxidase-conjugated secondary antibody. Signals were visualized by diaminobenzidine reaction and hematoxylin staining.

Western blot analysis for cells and tumor tissues

BGC-823 cells were seeded at 8×10^5 cells/well in 60 mm^2 plastic dishes. After incubation with DATS (50, 100 or 200 μmol/L) for 24 h, cells were washed with PBS and lysed in 150 μL cell lysis buffer. The tumors (30 mg) were homogenized in ice-cold cell lysis buffer (Solarbio Life Sciences) containing 1 mmol/L phenylmethylsulfonyl fluoride (PMSF, Sigma Aldrich, St Louis, MO, USA) and 1% cocktail protease inhibitors (Sigma). Total proteins were extracted by centrifugation and separated by 8%–15% SDS-PAGE. The proteins were then transferred on a polyvinylidene difluoride (PVDF) membrane, and the membranes were blocked in 5% skim milk for 2 h. The membranes were subsequently probed overnight with the appropriate primary antibodies at 4 °C. After washing, the membranes were exposed to HRP-conjugated secondary antibody (1:5000) for 1 h and washed again in TBST buffer. Final detection was performed by enhanced chemiluminescence system (Merck Millipore, Darmstadt, Germany). The signal intensity of each band was quantified using the Alphalmager HP system (Cell Biosciences, Inc, Santa Clara, CA, USA).

Statistical analysis

The data were presented as the mean±SEM. The statistical significance was assessed using analysis of variance (ANOVA) and a Student's *t*-test with Prism GraphPad 6.0 software. Values of $P<0.05$ were considered statistically significant.

Results

DATS suppressed cell viability, induced G_2/M phase cell cycle arrest and regulated related protein expression in BGC-823 cells

We estimated the effect of DATS on gastric cancer cell viability using the SRB assay. We also used the GSE-1 cell line to determine whether DATS has similar effects on normal gastric epithelial cells. DATS inhibited BGC-823 cell viability in a dose-dependent manner (Figure 1A), and the IC_{50} was 115.2±4.3 μmol/L after 24 h drug exposure. DATS had a lesser effect on GSE-1 cell viability than BGC-823 cells.

Based on the IC_{50} value of DATS in BGC-823 cells, we tested three concentrations of DATS (50, 100 and 200 μmol/L) and evaluated whether DATS decreased cell viability via induction of cell cycle arrest. As shown in Figure 1B, DATS treatment induced a dose-dependent accumulation of cells in the G_2/M phase and a corresponding decrease in the G_1 and S phase fraction. We also observed a hypodiploid DNA content peak (sub-G_1), which indicated the presence of apoptotic cells (Figure 1C). These results suggest that DATS induces cell cycle arrest in the G_2/M phase, which leads to decreased survival of BGC-823 cells.

To further characterize the changes in cell cycle distribution, we analyzed changes in cyclin expression patterns by Western blotting (Figure 1C). Cell cycle progression is tightly governed by the cell cycle control system, which consists of cyclin-dependent kinases (CDK), cyclins and CDK inhibitors (CDKIs)[10]. The DATS-induced decrease of cells in G_1 phase correlated well with a reduction in cyclin E1 protein levels. In parallel, activation of the G_2/M checkpoint was indicated by induction of the G_2/M checkpoint proteins cyclin B1 and A2, specifically at high DATS concentrations. We also observed a significant decrease in PCNA (proliferating cell nuclear antigen) expression, which is an essential factor in DNA replication and many other processes in eukaryotic cells. These results suggest that DATS exerts its anti-proliferative effects in BGC-823 cells by stabilizing the cell cycle at G_2 phase through regulation of intracellular cyclin levels.

DATS induced apoptosis by regulating Bcl-2 family protein expression in BGC-823 cells

Because we observed an obvious apoptosis sub-G_1 peak in cell cycle analysis, we determined the correlation between the growth inhibitory effect of DATS and apoptotic cell death. As shown in Figure 2A, DATS treatment significantly increased the fraction of apoptotic cells in a dose-dependent manner; the total percentage of early and late apoptotic cells was 37.5% in the case of 200 μmol/L DATS for 24 h. In contrast, only 0.5% of early and 1.1% of late apoptotic cells were detected in the control samples. These results suggest that DATS efficiently induces BGC-823 cell apoptosis.

Increasing evidence has indicated that the regulation of Bcl-2 family proteins is involved in apoptosis signaling pathways[11]. As shown in Figure 2B, Bax levels were up-regulated, whereas the levels of anti-apoptotic proteins (Bcl-2, Bcl-xl) were significantly down-regulated. Furthermore, the levels of p53 (a regulator of apoptosis) and cytochrome *c* were up-regulated, consistent with increased apoptosis.

DATS induced the activation of caspase-dependent mitochondrial pathways in BGC-823 cells

Some forms of regulated cell death, such as apoptosis, are precipitated by activation of the cysteine proteases of the caspase family, including caspase-8, -9 and -3[12]. Our data indicated that the cleaved caspase-8 and cleaved caspase-9 levels increased in DATS-treated BGC-823 cells, which are essential initiator caspases of extrinsic (death receptor-driven regulated) cell death. Although we did not observe active caspase-3 expression, DATS treatment decreased caspase-3 levels in a concentration-dependent manner (Figure 3). The levels of progressive cleavage products of poly (ADP-ribose) polymerase (cleaved-PARP) and caspase-7 also increased in a concentration-dependent manner. These results demonstrated that DATS induced apoptosis in BGC-823 cells partially

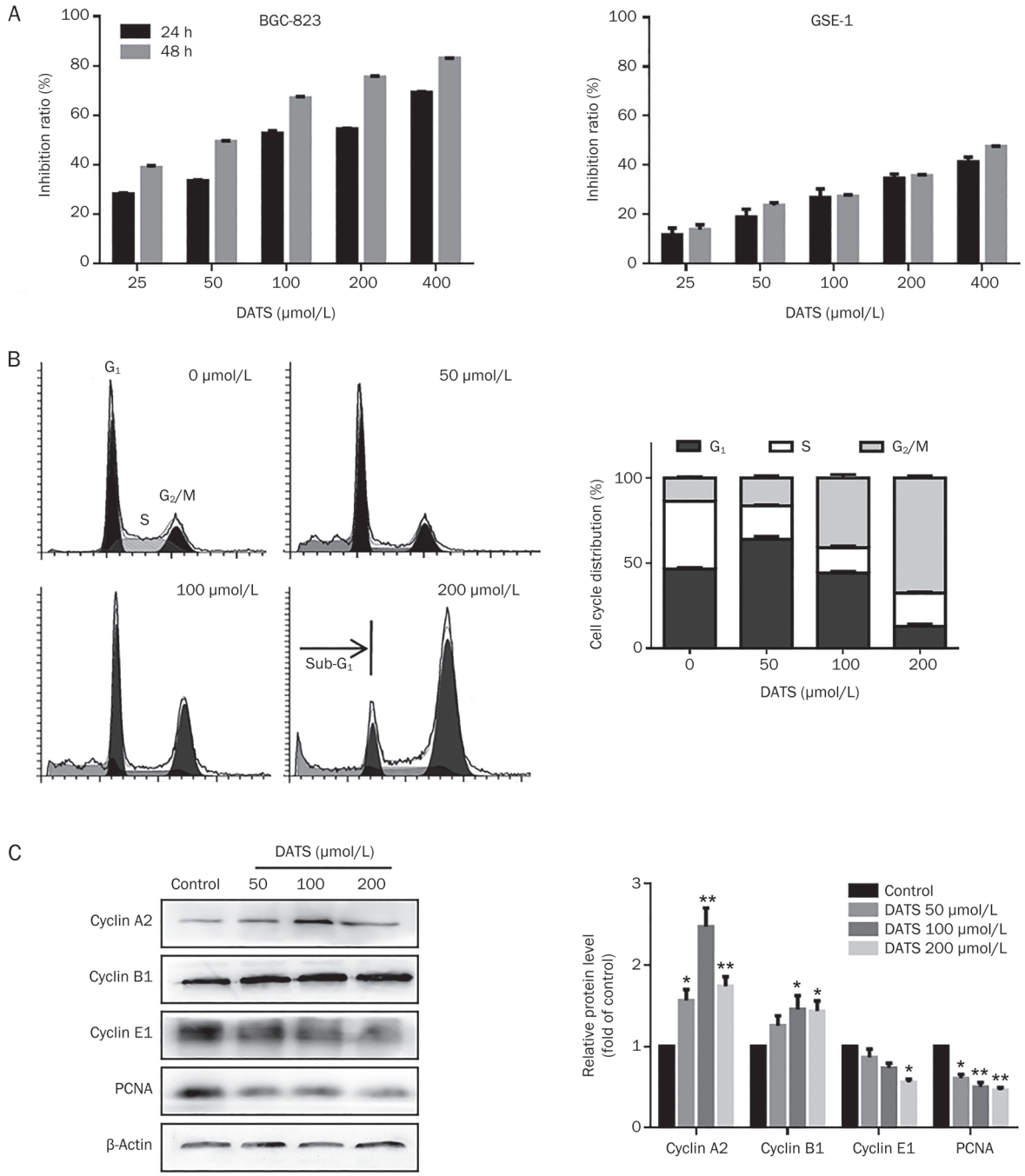

Figure 1. DATS suppressed cell viability, induced cell cycle G_2/M phase arrest and regulated cell cycle-related protein expression in BGC-823 cells. (A) Effects of DATS on viability in BGC-823 and GSE-1 cells. (B and C) PI staining and flow cytometric analysis were performed on BGC-823 cells after 24 h incubation at the indicated concentrations. Percentages of cells in the G_1, S and G_2/M phases, and representative images are indicated. (D) Representative Western blots from three individual experiments. Quantification analysis is shown for the effect of DATS treatment on cyclin expression in BGC-823 cells. The data are presented as the mean±SEM (n≥3). $^{*}P$<0.05, $^{**}P$<0.01.

through activation of the caspase pathway.

DATS inhibited tumor growth and enhanced DDP efficacy in a BGC-823 xenograft model

On the basis of our *in vitro* studies, we further examined the *in vivo* anti-cancer activities of DATS in a BALB/c nude mouse BGC-823 xenograft model. We administered DATS (at 20, 30 and 40 mg/kg) by intraperitoneal injection every day for 32 d after the xenograft tumor volume reached approximately 100 mm^3. As shown in Figure 4A, BGC-823 cell-derived xenograft tumors progressively grew in the control mice, whereas tumors grew more slowly in DATS-treated mice. DATS treatment significantly and dose-dependently reduced tumor volume and tumor weight (Figure 4C) compared to control mice (P<0.01

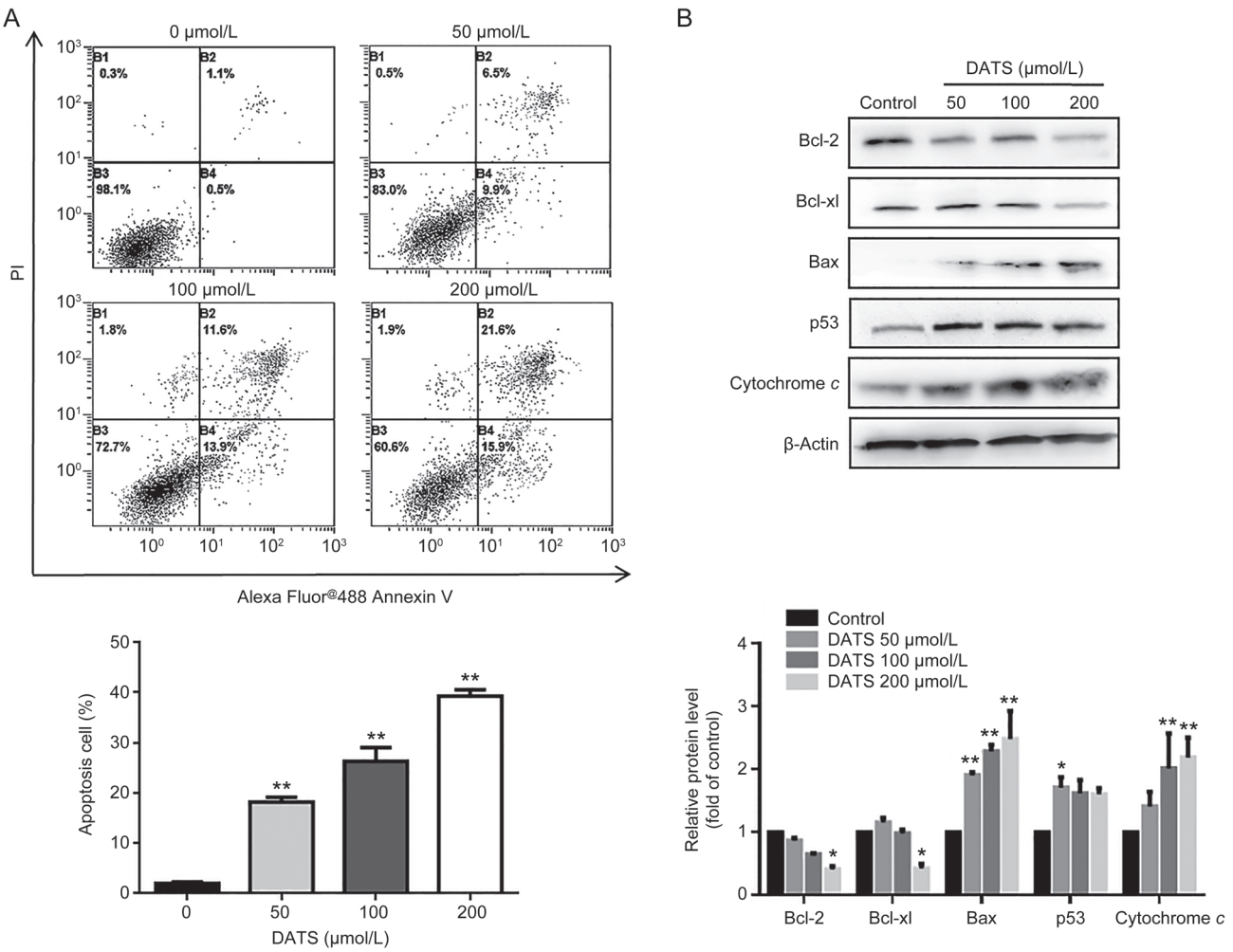

Figure 2. DATS induced BGC-823 cell apoptosis by regulating apoptosis-related protein expression. (A) Annexin V-FITC and PI staining and flow cytometry analysis for apoptosis were performed on BGC-823 cells after 24 h incubation with DATS at the indicated concentrations. Representative images from four independent experiments are indicated. The percentage of early and late apoptotic cells was analyzed by CXP software. (B) Western blot analysis of Bcl-2 family, p53 and cytochrome *c* protein expression after DATS treatment. The data are presented as the mean±SEM ($n \geq 3$). $^{*}P<0.05$, $^{**}P<0.01$.

for both tumor volume and weight). The positive DDP (5 mg/kg per 5 d) group demonstrated significant decreased tumor volumes (801.5±265.5 mm^3) and tumor weight (0.58±0.12 g) compared to the control group (1882.1±588.8 mm^3, 1.63±0.26 g, $P<0.01$ for both). However, DDP caused a significant decrease in body weight relative to the control group ($P<0.01$), which was suggestive of body damage. The DATS-treated group showed similar body weights to the control group. Therefore, we examined the effect of a combination of DDP and DATS (30 mg/kg) to investigate whether DATS could increase the efficacy of DDP and ameliorate the DDP-induced weight loss. As shown in Figure 4B and 4D, DDP+DATS treatment demonstrated further decreased tumor volume (664.0±148.4 mm^3) and tumor weight (0.42±0.06 g) compared to the mono-DDP therapy ($P<0.01$ for tumor volume). Interestingly, DATS+DDP treatment resulted in a notable increase in body weight compared to DDP treatment alone ($P<0.01$).

To further investigate the toxicity of DATS or DDP in nude mice, we collected and analyzed major organs (liver, kidney, lung and spleen) at the end of treatment. As shown in Figure 4E, DDP administration alone caused a significant reduction in spleen index compared to the control, and the combination of DDP and DATS significantly attenuated the decrease in spleen index. In addition, there were no significant losses in other organ indices in any of the groups, and all of the mice survived the treatment. Histopathological examination of the liver, kidney, lung and spleen revealed no obvious signs of toxicity to the tissues (data not shown).

DATS induced apoptosis and down-regulated Ki-67 expression in tumor tissues

To investigate the inhibition of tumor growth by DATS, we evaluated tumors for apoptosis and proliferation by H&E, TUNEL and Ki-67 staining. H&E staining revealed a substantial increase in tumor necrosis in the DATS treatment groups compared to the control group. TUNEL results further

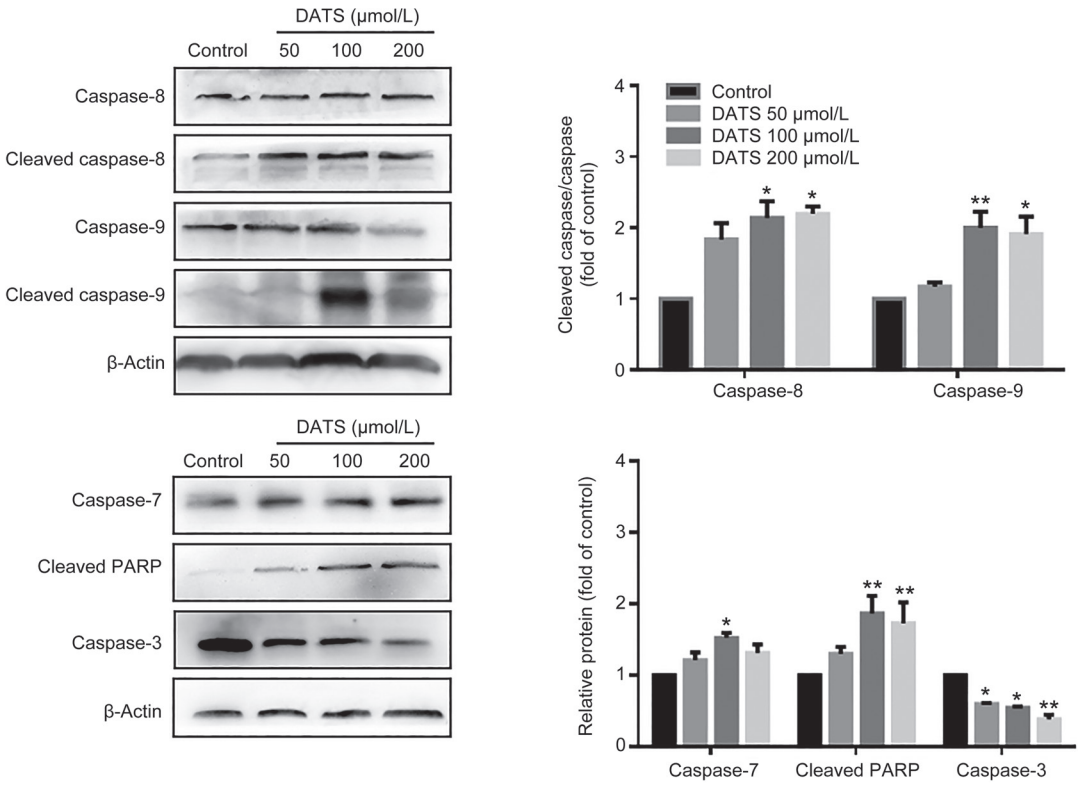

Figure 3. DATS activated the caspase pathway in BGC-823 cells. The level of caspase-related proteins in BGC-823 cells was measured by Western blot after 24 h of DATS treatment. The ratio of cleaved caspase and caspase, caspase-3/-7 and cleaved PARP protein expression was indicated. The data are presented as the mean±SEM (n≥3). $^{*}P$<0.05, $^{**}P$<0.01.

revealed that tumors in the DATS group had a significantly increased number of apoptotic cells, while the control group exhibited few TUNEL-positive cells. Ki-67 staining of BGC-823 tumor tissues dramatically decreased in the DATS groups compared to the control group. In addition, we observed significant expression changes in apoptosis proteins Bcl-2 and Bax in the tumors of DATS-treated mice (Figure 5B). We also observed a decrease in PCNA expression in DATS groups, which was consistent with the *in vitro* results.

Inactivation of Nrf2 and AKT kinases *in vitro* and *in vivo*

Nuclear factor erythroid 2-related factor 2 (Nrf2) is a key transcription factor that regulates antioxidant gene expression in response to oxidative stress or detoxification enzyme inducers[13, 14]. Nrf2 has recently emerged as an important factor in cancer therapy. As shown in Figures 6A and 7A, we observed a marked decrease in Nrf2 levels in the DATS-treated groups *in vitro* and *in vivo*. However, we did not observe significant changes in the downstream NAD(P)H:quinine oxidoreductase 1 (NQO1) level. In addition, it has been reported that the PI3K/Akt signaling pathway is involved in Nrf2 expression in anticancer therapy. As shown in Figure 6B and 7B, DATS suppressed Akt phosphorylation in both cells and tumors.

JNK and p38 kinase activation *in vitro* and *in vivo*

Mitogen-activated protein (MAP) kinases have important roles in numerous physiological and pathological processes, including inflammation stress, apoptosis, cell cycle and growth. It comprises ERK1/2 (p44/p42, extracellular signal-regulated kinase), JNK (c-Jun N-terminal kinase) and p38[15]. As shown in Figures 6B and 7B, administration of DATS led to a significant increase in p38 and JNK phosphorylation without any change in total protein levels *in vitro* and *in vivo*. In addition, DATS induced ERK phosphorylation *in vitro* but decreased ERK phosphorylation *in vivo* (Figure 6B). Taken together, DATS activated the MAPK pathways, especially JNK and p38 kinases in BGC-823 tumors.

Discussion

Cisplatin-based cytotoxic chemotherapy is widely used in gastric cancer, but its use is associated with significant side effects and low overall survival. The search for novel and advanced chemotherapeutic drugs or drug combinations is of the utmost importance. Remarkably, DATS is reported to be effective in different tumor types, but conclusive data on its effects in combination with cisplatin have not yet been reported. We thus focused on the anticancer mechanism of DATS on human gastric cancer cells and evaluated whether DATS enhanced the efficacy of DDP while improving quality of life in a nude mouse xenograft model.

The present study shows that DATS significantly suppressed gastric cancer cell proliferation, with less effect on nor-

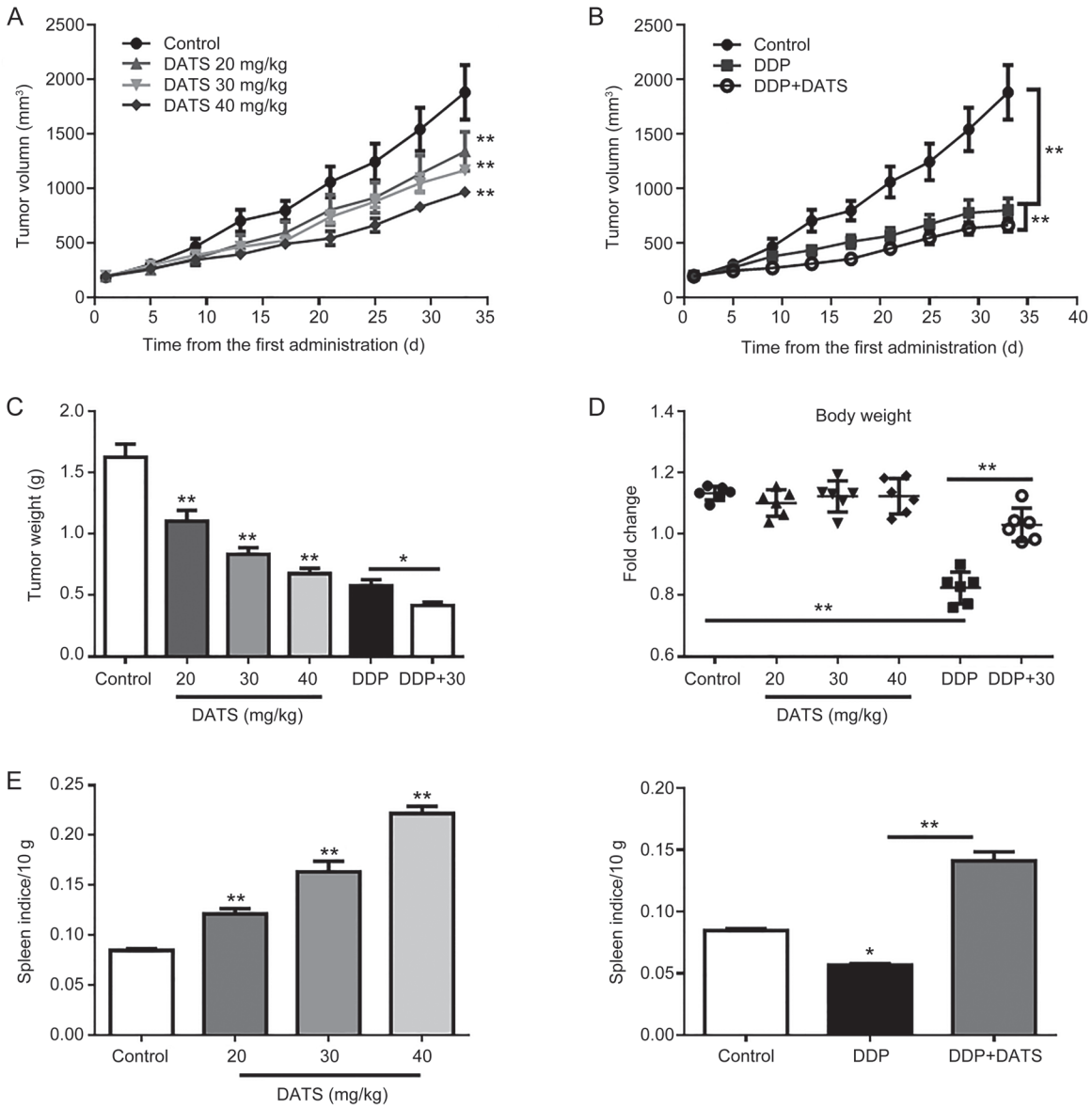

Figure 4. Anti-tumor activity of DATS alone and DATS combined with DDP in BGC-823 xenograft tumors. Tumor-bearing mice (6 animals per group) were treated by intraperitoneal injection, as follows: vehicle control, DATS (20, 30, 40 mg·kg^{-1}·d^{-1}), DDP (5 mg·kg^{-1}·5d^{-1}) and a combination of DDP and DATS (30 mg/kg) for 32 d. (A and B) Average tumor volume for each group. (C) Tumor weight for each group at the end of the observation period. (D) Change in body weight for each group. (E) The spleen indices for each group are indicated. Weight$_{(spleen)}$/Weight$_{(body)}$×10 g. The values represent the mean±SEM (n=6). $^{*}P$<0.05, $^{**}P$<0.01.

mal gastric GSE-1 cell proliferation. In response to increased concentrations of DATS, the intracellular expression of apoptosis-related proteins were significantly activated in BGC-823 cells. Bcl-2 family members and caspase members are crucial mediators of apoptosis[11, 12]. Among Bcl-2 family proteins, DATS treatment decreased anti-apoptotic proteins Bcl-2 and Bcl-xl, increased apoptotic protein Bax and promoted cytochrome *c* release, which enhanced apoptosis. In caspase-dependent apoptosis, DATS contributed to the production of several cleaved caspase substrates (caspase-8/-9), which led to caspase cascade activation. Caspase-3 and caspase-7 catalyzed native PARP processing to the cleaved form, indicating that DATS induced apoptosis partly through the mitochondrial cell death pathway. Additionally, we observed a reduction of DNA replication in S-phase and accumulation of cells in the G_2/M phase, which blocked cell cycle progression. These findings together suggested that the DATS regimen is a potential strategy for cancer treatment.

To dissect the molecular factors underlying the anticancer efficacy of DATS, we analyzed the cellular stress signal pathways. In general, the MAPK family is considered to be redox-regulated, and its activation has been correlated with the induction of apoptosis. JNK phosphorylation has been reported to regulate the activity of Bcl-2 family members, such

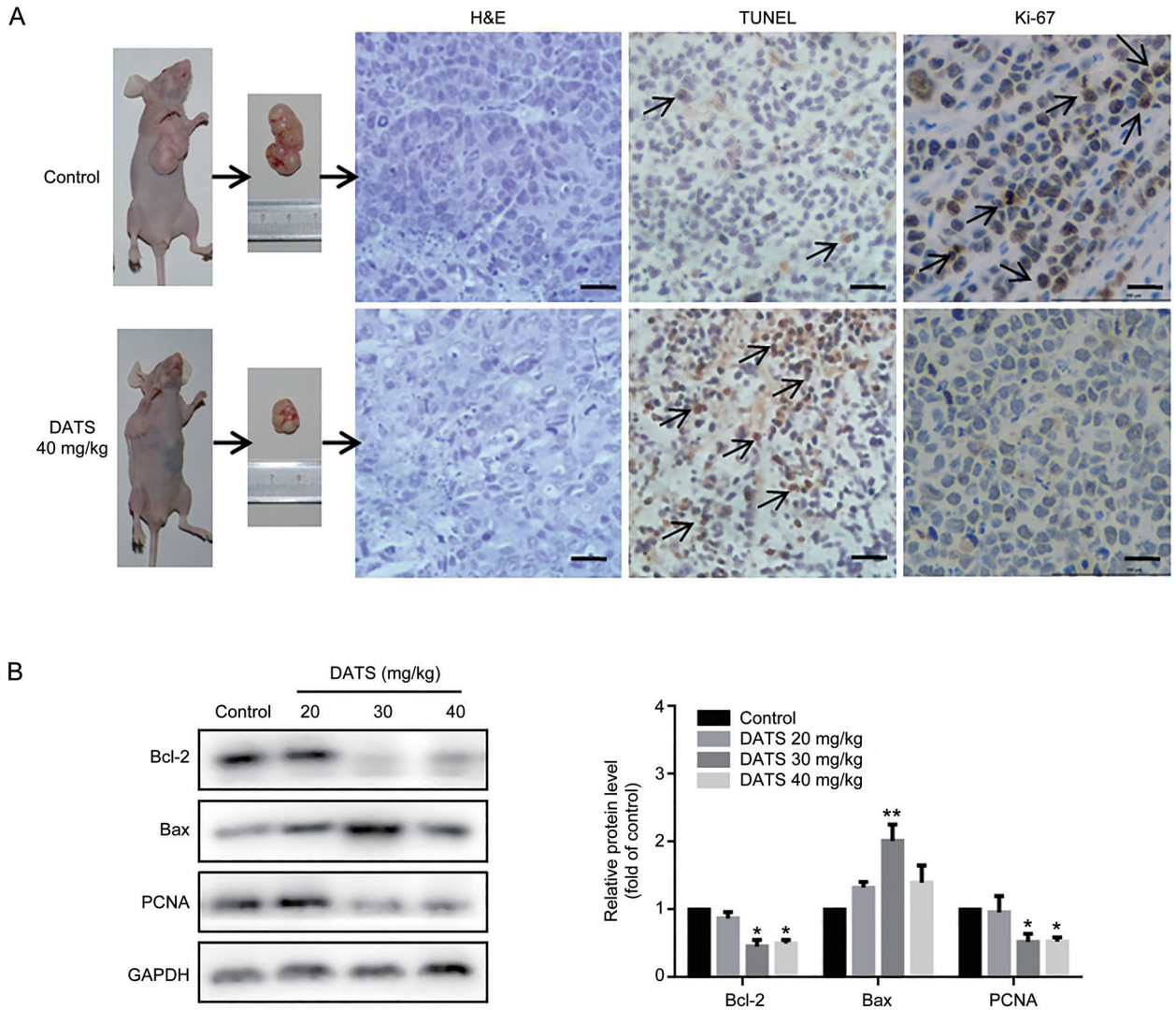

Figure 5. DATS treatment induced apoptosis in BGC-823 xenograft tumors. (A) Representative micrographs of tumor sections in control and DATS (40 mg/kg) groups: H&E staining, TUNEL staining and Ki-67 IHC. Scale bar=20 μm. (B) Western blot analysis of apoptotic (Bcl-2 and Bax) and cell cycle (PCNA) markers in tumor tissues. The data are presented as the mean±SEM (n=3). $^{*}P<0.05$, $^{**}P<0.01$ (versus the control group).

as Bcl-2, Bax, Bcl-xl, in response to a variety of extracellular stimuli[16]. For example, activation of JNK-mediated multisite phosphorylation of Bcl-2 has been confirmed in diallyl tetrasulfide-induced U937 cells, which represents the missing link between early mitotic arrest and the onset of apoptosis[17]. In MCF-7 cells, DATS induced apoptosis through JNK activation and Bcl-2 phosphorylation[18]. Previous studies have shown that p38 MAPK and JNK phosphorylation induced caspase-3, -8 and -9 activation[19, 20], leading to caspase-independent cell death in tumor cells. The results of this study showed that activation of p-JNK significantly modulated the ratio of anti- and pro-apoptotic protein expression (Bcl-2/Bax) in DATS-induced cancer cells and tumors. Additionally, activated JNK and p38 phosphorylate numerous proteins involved in caspase family activation to ultimately lead to cell growth and decreased apoptosis. The expression of p-ERK MAPK increased in response to DATS treatment *in vitro*, but decreased *in vivo*, which suggests that the role of ERK requires further investigation.

Nrf2, a redox-sensitive transcription factor in the antioxidant and cytoprotective response, has emerged as an important regulator of tumor proliferation, invasion, and chemoresistance activities of various cancer cells[21, 22]. The PI3K/Akt signaling pathway is a crucial regulator of several cell processes, including proliferation, differentiation and metastasis[23]. Evidence has shown that Nrf2 and the expression of its downstream genes was regulated through the phosphatidylinositol-3 kinase (PI3K)/Akt pathway[24, 25]. Our data showed marked dose-dependent reductions in Akt phosphorylation and Nrf2 expression in DATS-treated cells, which we also confirmed *in vivo*.

Based on our *in vitro* and *in vivo* results, DATS treatment alone exhibited excellent anti-tumor activity with fewer side effects. Interestingly, recent studies have demonstrated that

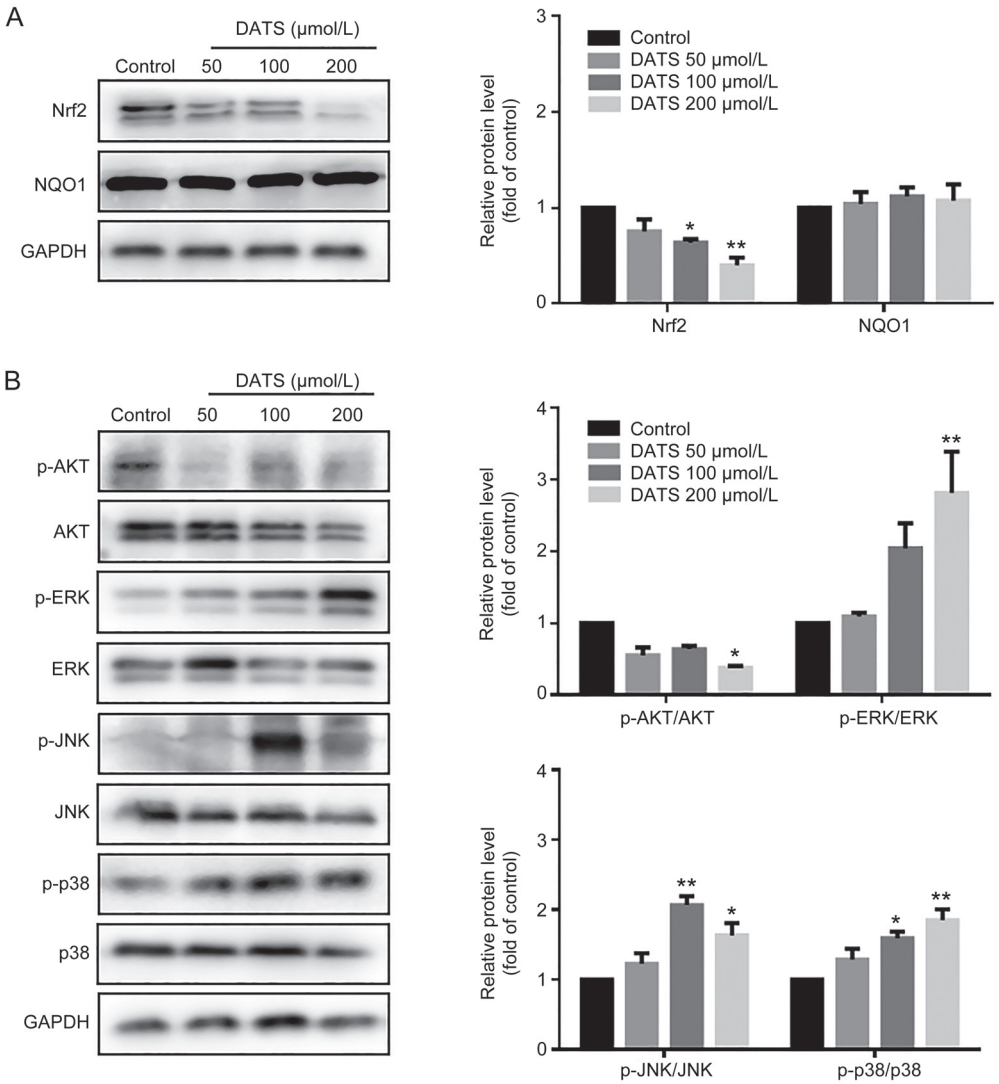

Figure 6. DATS modulated the Nrf2/Akt and MAPK pathway in BGC-823 cells. The levels of Nrf2, NQO1, Akt and MAPK family in DATS-treated BGC-823 cells were measured by Western blot. The ratio of phosphorylated and total protein was indicated. The data are presented as the mean±SEM ($n \geq 3$). $^{*}P<0.05$, $^{**}P<0.01$.

in combination with docetaxel, DATS exhibited synergistic anti-gastric cancer activity accompanied by MT2A upregulation and NF-κB inactivation[26]. DATS possesses potent *in vitro* fungicidal effects, and its activity was synergistic with that of amphotericin B[27]. Additionally, aged garlic extract in combination with DDP has demonstrated prevention and anti-inflammation effects[28]. Therefore, DATS in combination with DDP may be a more efficient and less toxic therapeutic strategy.

We analyzed the *in vivo* antitumor effect of DATS in a BGC-823 xenograft tumor model. We observed an apparent decrease in tumor volume in DATS-treated mice compared to controls. Meanwhile, we observed a significant inhibition of proliferation in DATS-treated mice based on Ki-67 immunohistochemistry. Of note, DATS treatment did not affect the liver, kidney or total body weight. We further investigated the antitumor effect of DATS in combination with DDP. Interestingly, compared to DDP alone, DATS+DDP treatment significantly inhibited tumor growth and reduced weight loss. We found that spleen indices were significantly decreased in the DDP alone treatment but increased in the DDP+DATS group, which suggested that immune-modulation might play a role during DATS and DDP combination therapy. Nevertheless, the exact mechanism requires further investigation.

The results from the present study clearly indicate that multiple pathways are involved in DATS-mediated antitumor activity, including JNK/p38 and Nrf2/Akt. In BGC-823 cells, JNK/p38 MAPK proteins played an important role in the DATS-induced antitumor activity through the regulation of cell progression and induction of cell apoptosis. Furthermore, MAPK proteins also modulated Bcl-2 and caspase family members, which are crucial regulators of cell apoptosis. Furthermore, DATS dramatically reduced Nrf2 protein expression *in vitro* and *in vivo*, accompanied with down-regulation of Akt

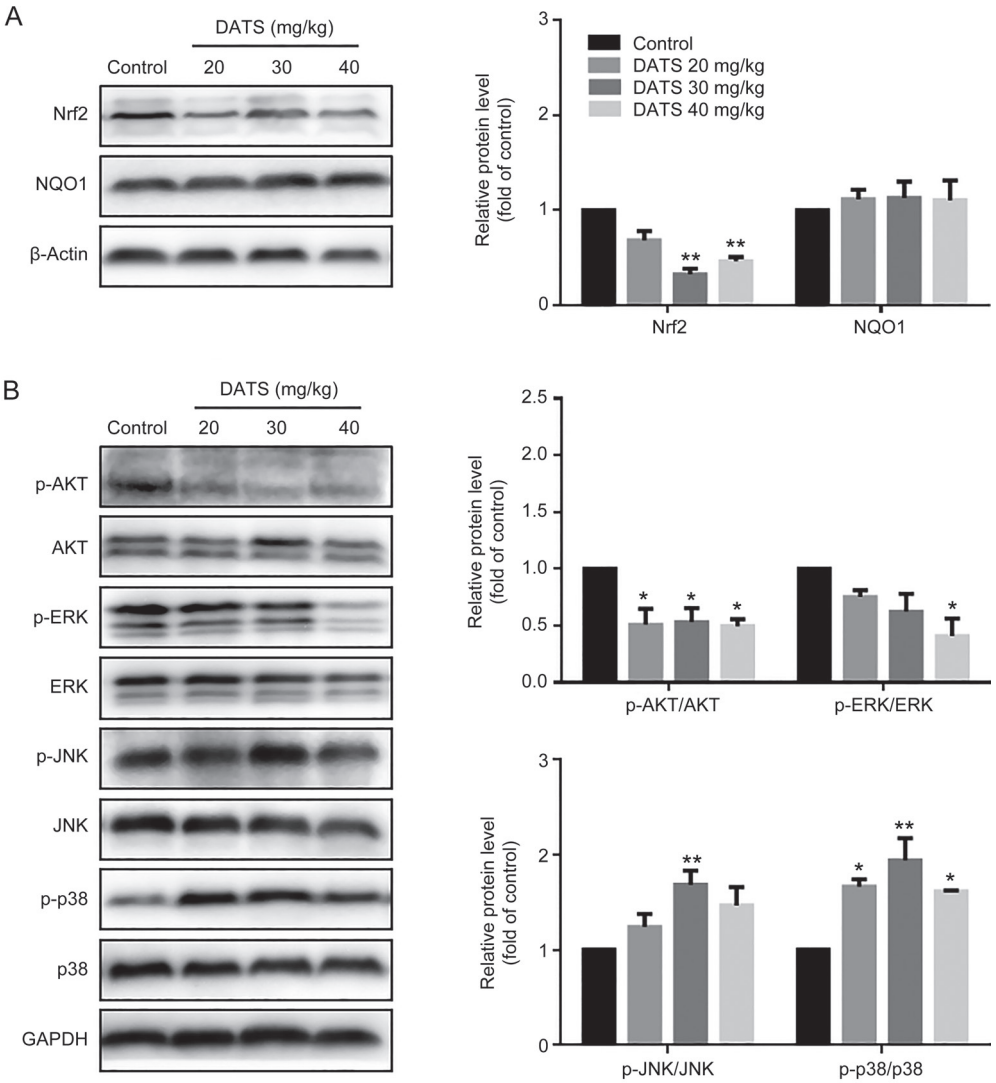

Figure 7. Modulation of intracellular signaling molecules involved in tumor inhibition in BGC-823 tumor tissues. (A) Effect of DATS on Nrf2 and NQO1 expression. (B) Effect of DATS on the expression of phosphorylated and total Akt, ERK1/2, JNK and p38. The data are presented as the mean±SEM (n=3), $^{*}P$<0.05, $^{**}P$<0.01 (versus the control group).

phosphorylation. However, Nrf2 plays dual roles in cancer prevention and progression depending on the cellular context and environment. A better understanding of Nrf2 will be necessary to explore this balance in antioxidant pathways and inhibition of tumor progression.

In conclusion, we suggest that DATS suppresses gastric cancer through attenuation of Nrf2/Akt and activation of the JNK and p38-MAPK pathways, highlighting a potential mechanism for DATS activity, which may be used as a therapeutic agent for gastric cancer. Finally, this study also provides evidence that the combination of DATS and DDP enhances the anticancer efficacy in gastric cancer.

Acknowledgements

This work was supported by the funds from National "Major Science and Technology Project–Prevention and Treatment of AIDS, Viral Hepatitis, and Other Major Infectious Diseases" (Grant No 2013ZX10005004), Major Project of Science and Technology of Shandong Province (Grant No 2015ZDJS04001), Science & Technology Enterprise Technology Innovation Fund of Jiangsu Province (Grant No BC2014172), Small & Medium Enterprise Technology Innovation Project of Lianyungang City (Grant No CK1333).

Author contribution

Zhong-xi ZHAO and Si-ying LI conceived of and designed the experiment; Xiao-yan JIANG, Xiao-song ZHU, and Hong-ya XU performed the experiments and analyzed the data; Shan-zhong LI, Jian-hua CAI, and Ji-min CAO provided the reagents, materials and analysis tools; Xiao-yan JIANG wrote the paper.

References

1 Siegel R, Naishadham D, Jemal A. Cancer statistics, 2013. CA Cancer J Clin 2013; 63: 11–30.
2 Fleischauer AT, Poole C, Arab L. Garlic consumption and cancer prevention: meta-analyses of colorectal and stomach cancers. Am J Clin Nutr 2000; 72: 1047–52.
3 Powolny AA, Singh SV. Multitargeted prevention and therapy of cancer by diallyl trisulfide and related Allium vegetable-derived organosulfur compounds. Cancer Lett 2008; 269: 305–14.
4 Chandra-Kuntal K, Lee J, Singh SV. Critical role for reactive oxygen species in apoptosis induction and cell migration inhibition by diallyl trisulfide, a cancer chemopreventive component of garlic. Breast Cancer Res Treat 2013; 138: 69–79.
5 Antony ML, Singh SV. Molecular mechanisms and targets of cancer chemoprevention by garlic-derived bioactive compound diallyl trisulfide. Indian J Exp Biol 2011; 49: 805–16.
6 Lai KC, Hsu SC, Yang JS, Yu CC, Lein JC, Chung JG. Diallyl trisulfide inhibits migration, invasion and angiogenesis of human colon cancer HT-29 cells and umbilical vein endothelial cells, and suppresses murine xenograft tumour growth. J Cell Mol Med 2015; 19: 474–84.
7 Ozkok A, Edelstein CL. Pathophysiology of cisplatin-induced acute kidney injury. Biomed Res Int 2014; 2014: 967826.
8 Ashraf YN, Amal ASI. Aged garlic extract ameliorates the oxidative stress, histomorphological, and ultrastructural changes of cisplatin-induced nephrotoxicity in adult male rats. Microsc Res Tech 2015; 78: 452–61.
9 Schäfer G, Kaschula CH. The immunomodulating and anti-inflammatory effects of garlic organosulfur compounds in cancer prevention. Anticancer Agents Med Chem 2014; 14: 233–40.
10 Hydbring P, Malumbres M, Sicinski P. Non-canonical functions of cell cycle cyclins and cyclin-dependent kinases. Nat Rev Mol Cell Biol 2016; 17: 280–92.
11 Yip KW, Reed JC. Bcl-2 family proteins and cancer. Oncogene 2008; 27: 6398–406.
12 Olsson M, Zhivotovsky B. Caspases and cancer. Cell Death Differ 2011; 18: 1441–9.
13 Hayes JD, Dinkova-Kostova AT. The Nrf2 regulatory network provides an interface between redox and intermediary metabolism. Trends Biochem Sci 2014; 39: 199–218.
14 Xiang Y, Kensler T. Nrf2 as a target for cancer chemoprevention. Mutat Res 2005; 591: 93–102.
15 Kyriakis JM, Avruch J. Mammalian MAPK signal transduction pathways activated by stress and inflammation: a 10-year update. Physiol Rev 2012; 92: 689–737.
16 Wei Y, Sinha SC, Levine B. Dual role of JNK1-mediated phosphorylation of Bcl-2 in autophagy and apoptosis regulation. Autophagy 2008; 4: 949–51.
17 Kelkel M, Cerella C, Mack F, Schneider T, Jacob C, Schumacher M*, et al.* ROS-independent JNK activation and multisite phosphorylation of Bcl-2 link diallyl tetrasulfide-induced mitotic arrest to apoptosis. Carcinogenesis 2012; 33: 2162–71.
18 Na HK, Kim EH, Choi MA, Park JM, Kim DH, Surh YJ. Diallyl trisulfide induces apoptosis in human breast cancer cells through ROS-mediated activation of JNK and AP-1. Biochem Pharmacol 2012; 84: 1241–50.
19 Zhuang S, Demirs JT, Kochevar IE. p38 mitogen-activated protein kinase mediates bid cleavage, mitochondrial dysfunction, and caspase-3 activation during apoptosis induced by singlet oxygen but not by hydrogen peroxide. J Biol Chem 2000; 275: 25939–48.
20 Harada J, Sugimoto M. An inhibitor of p38 and JNK MAP kinases prevents activation of caspase and apoptosis of cultured cerebellar granule neurons. Jpn J Pharmacol 1999; 79: 369–78.
21 Singh A, Boldinadamsky S, Thimmulappa RK, Rath SK, Ashush H, Coulter J*, et al.* RNAi mediated silencing of Nrf2 gene expression in non-small cell lung cancer inhibits tumor growth and increases efficacy of chemotherapy. Cancer Res 2008; 68: 7975–84.
22 Wang XJ, Sun Z, Villeneuve NF, Zhang S, Zhao F, Li Y*, et al.* Nrf2 enhances resistance of cancer cells to chemotherapeutic drugs, the dark side of Nrf2. Carcinogenesis 2008; 29: 1235–43.
23 Fresno Vara JA, Casado E, de Castro J, Cejas P, Belda-Iniesta C, González-Barón M. PI3K/Akt signalling pathway and cancer. Cancer Treat Rev 2004; 30: 193–204.
24 Gao AM, Ke ZP, Wang JN, Yang JY, Chen SY, Chen H. Apigenin sensitizes doxorubicin-resistant hepatocellular carcinoma BEL-7402/ADM cells to doxorubicin via inhibiting PI3K/Akt/Nrf2 pathway. Carcinogenesis 2013; 34: 1806–14.
25 Liu D, Zhang Y, Wei Y, Liu G, Liu Y, Gao Q*, et al.* Activation of AKT pathway by Nrf2/PDGFA feedback loop contributes to HCC progression. Oncotarget 2016; 7: 65389–402.
26 Pan Y, Lin S, Rui X, Min Z, Lin B, Cui J*, et al.* Epigenetic upregulation of metallothionein 2A by diallyl trisulfide enhances chemosensitivity of human gastric cancer cells to docetaxel through attenuating NF-κB activation. Antioxid Redox Signal 2016; 24: 839–54.
27 Shen J, Davis LE, Wallace JM, Cai Y, Lawson LD. Enhanced diallyl trisulfide has *in vitro* synergy with amphotericin B against *Cryptococcus neoformans*. Planta Med 1996; 62: 415–8.
28 Nasr AY, Saleh HA. Aged garlic extract protects against oxidative stress and renal changes in cisplatin-treated adult male rats. Cancer Cell Int 2014; 14: 92.